ARTICLE
Journal of Cellular Biochemistry 111:955–966 (2010)

Journal of Cellular Biochemistry

Fullerene–Polyvinylpyrrolidone Clathrate Localizes in the Cytoplasm to Prevent Ultraviolet-A Ray-Induced DNA-Fragmentation and Activation of the Transcriptional Factor NF-kappaB

Li Xiao,[1] Hisae Aoshima,[2] Yasukazu Saitoh,[1] and Nobuhiko Miwa[1*]

[1] *Laboratory of Cell-Death Control BioTechnology, Faculty of Life and Environmental Sciences, Prefectural University of Hiroshima, Nanatsuka 562, Shobara, Hiroshima 727-0023, Japan*

[2] *Vitamin C60 BioResearch Corporation, Tatsunuma Tatemono Bldg. 9F 1-3-19 Yaesu, Chuo-ku, Tokyo 103-0028, Japan*

ABSTRACT

By Western blot and immunostaining we proved that polyvinylpyrrolidone (PVP)-wrapped fullerene molecules (PVP–fullerene) could combine the 8- and 53-kb proteins which localize in the membrane of human skin keratinocytes HaCaT. Only fullerene molecules are able to cross the lipid membrane and conjugate 53-kb proteins in the cytosol. There are no fullerene molecules detectable in the nucleus or cytoskeleton. Ultraviolet-A (UVA)-irradiation on HaCaT or normal human epidermal melanocytes (NHEM) caused nuclear fragmentations, lowering of intracellular DNA-contents below diploidy, concurrently with the repressed DNA synthesis and the increased DNA-3′OH cleavage terminals, all of which were repressed by PVP–fullerene, as shown by flow cytometry and PI- or TUNEL-stain fluorography. Translocation of the transcriptional factor NF-kappaB in the cytoplasm to the nucleus of the keratinocytes was caused with UVA and repressed by PVP–fullerene with cytoprotective effects. Thus, the PVP–fullerene may be developed as a UV-protective agent with DNA-preservative effects owing to its combinative ability to molecules in the cytoplasm and cytomembrane, and then represses cellular oxidative stress and blocks abnormal signal pathways. J. Cell. Biochem. 111: 955–966, 2010.

KEY WORDS: FULLERENE; CELLULAR-BINDING SITE; UVA; APOPTOSIS; NF-kappaB

The interaction of fullerene (C60) or its water-soluble derivatives with various biological systems, such as organs, tissues, cells, and cellular molecules has recently become an issue of great research interest. Fullerenes have been characterized as novel powerful antioxidants and new radical-scavenging compounds, and are believed to protect various types of cells, tissues, and organs from oxidative stress causing injuries, without acute and subacute toxicities. Increasing evidences demonstrated that cytoprotective activities of water-soluble fullerenes are considered to ensue from their ability to pass the bio-membranes and then scavenge the harmful free radicals or reactive oxygen species (ROS) [Krusic et al., 1991; Dugan et al., 1996; Lin et al., 1999; Hu et al., 2007; Witte et al., 2007]. It is considered that fullerene C60 molecule has a high potential for permeability into bilayer membrane because it is not hydrophilic. It has also a high solubility in the lipid core and strong attractive interactions with the outer layer of the membrane [Bedrov et al., 2008]. A computer simulation study suggested that the fullerene C60 molecules rapidly aggregate in water but disaggregate after entering the membrane interior. High concentrations of fullerene induce changes in the structural and elastic properties of the lipid bilayer, but there is no mechanical damage in the membrane [Wong-Ekkabut et al., 2008]. When the pristine C60 was taken up into cells, crystals, or aggregates were observed in close proximity to the cell membrane as well as in the cytoplasm, along the nuclear membrane and within the nucleus [Porter et al., 2006]. However, for fullerene derivatives, the permeability depends on the molecular size, lipophilicity, and hydrophilic bond moieties [Lipinski et al., 2001]. The mechanism of uptake of fullerenes into cells is considered to include two main pathways: diffusion- and the receptor-mediated endocytosis. The immune repertoire could recognize and process fullerenes as protein conjugates [Chen et al., 1998]. An in vivo study showed that a water-miscible fullerene

*Correspondence to: Nobuhiko Miwa, Laboratory of Cell-Death Control BioTechnology, Faculty of Life and Environmental Sciences, Prefectural University of Hiroshima, Nanatsuka 562, Shobara, Hiroshima 727-0023, Japan.
E-mail: miwa-nob@pu-hiroshima.ac.jp

Received 8 June 2010; Accepted 15 July 2010 • DOI 10.1002/jcb.22784 • © 2010 Wiley-Liss, Inc.
Published online 27 July 2010 in Wiley Online Library (wileyonlinelibrary.com).

(trimethylenemethane–fullerene) distributes rapidly in many tissues and is able to cross the blood–brain barrier by intravenous injection in rats [Yamago et al., 1995]. An orally administered water-soluble fullerene derivative C3 (e,e,e-C60(C(COOH)$_2$)$_3$) can penetrate the nervous system, significantly increase lifespan of mice and reduce mitochondrial free radical production in the brain [Quick et al., 2008]. C60(C(COOH)2)2 nanoparticles could selectively enter oxidation-damaged cerebral endothelial cells and maintain their integrity, then protect the cells from hydrogen peroxide-induced apoptosis [Lao et al., 2009].

Chronic exposure to ultraviolet light A (UVA) (320–380 nm) causes DNA damages to skin cells, and is then followed by immunosuppression, photodermatoses, photoaging, and photocarcinogenesis [Ashok et al., 1998; Valko et al., 2007; Ridley et al., 2009]. Nuclear transcriptional factor kappaB (NF-kappaB) is involved in most of the above-mentioned UVA-mediated biological processes via ROS [Tyrrell, 1996; Tak and Firestein, 2001]. UVA-induced ROS formation rapidly releases labile irons, which mediate lipid peroxidation in cell membranes, and consequently cause increases in permeability of nuclear membrane. This iron-induced lipid peroxidation in cell membranes is the main contributor to induction of NF-kappaB [Reelfs et al., 2004]. NF-kappaB plays a central role in cell death-signaling cascades-related factors such as TNF, TRAIL, IL-1, JNK, bcl-2, and TGF-beta, all of which are related to apoptotic signaling pathway [Yanada et al., 2006; Gan et al., 2009; Plantivaux et al., 2009; Testa, 2010]. NF-kappaB acts as an anti-apoptotic factor in TRAIL- and CD95-induced apoptosis through TNF-alpha and IL-1 signaling pathway [Kothny-Wilkes et al., 1998, 1999]. However, UVA- and UVB-induced DNA damages appear to cause the conversion of NF-kappaB from an anti-apoptotic mediator to a mediator of proapoptotic pathways by changing its transcriptional properties, consequently enhancing UV-induced apoptosis [Pöppelmann et al., 2005; Strozyk et al., 2006]. Therefore, to protect skin cells from UVA-induced apoptosis, potential reagents should have abilities to (1) scavenge cellular ROS, (2) stabilize cellular membranes, especially nuclear membrane, and (3) reduce NF-kappaB activation.

It has been reported that fullerene C60 and water-soluble fullerene derivatives could be used as antioxidants against radical-initiated lipid peroxidation [Wang et al., 1999; Hu et al., 2007; Yin et al., 2009; Xiao et al., 2010]. By this reason, fullerenes might be good candidates to be cytoprotective against UVA-induced apoptosis. In our previous study, we had successfully prepared a hydrophilic polymer-wrapped fullerene from purified fullerene BioFullerene® and polyvinylpyrrolidone (PVP), designated as PVP–fullerene. PVP–fullerene showed the excellent antioxidant effects as a free radical scavenger in terms of the molecular and cellular levels, and protected skin cells from UVA-, UVB-, and the hydroperoxide t-BuOOH-mediated cell death. PVP–fullerene markedly scavenged UVA-induced ROS inside human melanocytes [Xiao et al., 2005, 2006, 2007]. In the present study, to investigate the anti-apoptotic effect of PVP–fullerene, we examined its distribution inside/outside the cell after administration and its effects on UVA-irradiation-induced apoptosis, DNA strand cleavages, and NF-kappaB translocation in skin keratinocytes and melanocytes.

MATERIALS AND METHODS

PREPARATION OF PVP–FULLERENE

PVP–fullerene is composed of the purified fullerene-C_{60}, BioFullerene® (Vitamin C60 BioResearch, Inc., Tokyo) and PVP of 60–80 kDa at a mixing molar ratio range of 0.42–0.67:1. PVP-entrapped BioFullerene® was prepared as the previous report [Xiao et al., 2006].

CELL CULTURE

Human skin epidermal keratinocytes HaCaT were kindly provided from Prof. Norbert E. Fusenig of Deutsches Krebsforschungszentrum (Heidelberg, Germany) [Boukamp et al., 1988], and cultivated as previously described [Xiao et al., 2005]. Normal human skin epidermal melanocytes (NHEM) were purchased from Kurabo Bio. Int., Osaka and maintained according to the manufacturer's protocol. The culture medium was replaced by fresh medium for every 48 h before the experiment.

IMMUNOFLUORESCENCE STAIN

Cells were seeded in a four-well Lab-Tek chamber slide. After treatment, the cells were fixed for 5 min in −10°C methanol, and air dried. Specimens were incubated with 10% skim milk in calcium- and magnesium-free PBS for 20 min to suppress non-specific binding of IgG, and then incubated for 60 min with anti-NF-kappaB rabbit polyclonal IgG (sc-109, Santa Cruz, Inc.), anti-fullerene-C60, or anti-PVP–fullerene rabbit polyclonal IgG primary antibody (1:100 dilution in 1.5% skim milk in PBS). Specimens were stained with the FITC-conjugated goat anti-rabbit IgG (sc-2012, Santa Cruz, Inc.) secondary antibody (diluted to 1–5 μg/ml in 1.5% skim milk in PBS) in dark for 45 min. The fluorescence images of stained cells were observed under a fluorescence microscope and photographed using an ACT-II software (Nikon ECLIPSE E 600, Nikon Co., Tokyo).

PREPARATION OF ANTI-BIOFULLERENE AND ANTI-PVP–FULLERENE POLYCLONAL ANTIBODY

Two rabbits were immunized four times with Biofullerene or PVP–fullerene using a combination of Freund's complete adjuvants. On 24 and 36 days after the first immunization, the enzyme-linked immunosorbent assay (ELISA) was performed in substrate plates which were coated with Biofullerene or PVP–fullerene at a concentration of 10 or 2,400 μg (containing ~8 μg Biofullerene)/ml, respectively. The developed color was measured spectrophotometrically at 405 nm. The serum ELISA titer was markedly raised by Biofullerene or PVP–fullerene antigen with 1:10 diluted antisera on 24 and 36 days after the first immunization (Fig. 1). On 36 days after, the rabbits were subjected to exsanguination and the subsequent immunofluorescence studies were done with this antiserum.

WESTERN BLOTTING

Cellular-binding sites of PVP–fullerene in HaCaT cells were detected by Western blotting analysis using the NuPAGE electrophoresis system from Invitrogen, Inc. Subcellular proteins of cytosol, membrane/organelle, nucleus, and cytoskeleton were extracted from adherent HaCaT cells by ProteoExtract® Subcellular Proteome

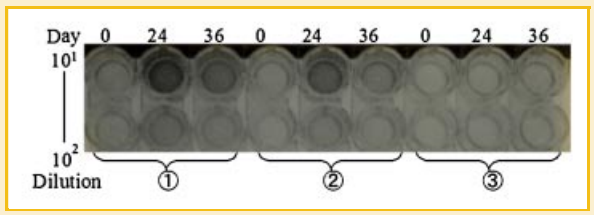

Fig. 1. Titration of anti-PVP–fullerene or anti-Biofullerene antiserum. ELISA was conducted on a 24-well microplate which was coated with: (1) PVP–fullerene antigen; (2) Biofullerene antigen; (3) Blank, and added sequentially with each antiserum and the secondary antibody followed by chemiluminescence.

Extraction Kit according to the detailed protocol (Calbiochem cat# 539790, EMD Chemicals, Inc., Germany). Protein concentration was determined by Bradford assay kit (Bio-Rad, Hercules, CA). Twenty micrograms of extracted proteins was separated according to their molecular weight using denaturing polyacrylamide gel electrophoresis (PAGE) by a NuPAGE 4–12% Bis-Tris gel (NP0322, Invitrogen, Inc.) and transferred to polyvinylidene fluoride membrane (IB4010-02, Invitrogen, Inc.). The immunodetection process was performed with a Novex® ECL Chemiluminescent Substrate Reagent Kit (WB20005, Invitrogen, Inc.) [Penna and Cahalan, 2007].

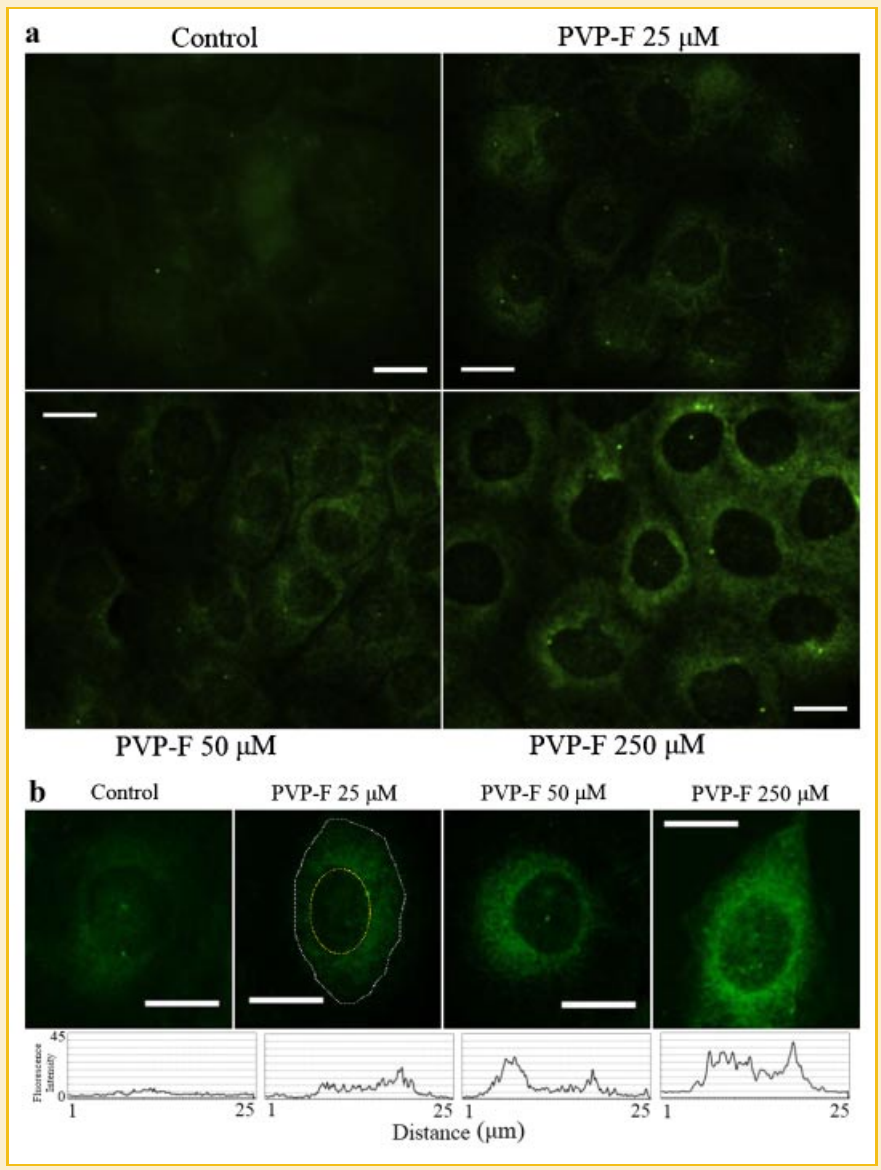

Fig. 2. Intracellular distribution of fullerene in human keratinocytes HaCaT. a: HaCaT cells were incubated with PVP–fullerene at different concentrations for 3 h, immunostained with anti-Biofullerene antiserum, and visualized with FITC-conjugated goat anti-rabbit IgG antibody. Specimens were observed under fluorescence microscope. The images are representatives of three independent experiments. PVP-F: PVP–fullerene (the following are identical). Scale bar = 10 μm. b: Intracellular distribution of fullerene in a single cell out of HaCaT cells treated as in (a). The histogram of the fluorescence intensity corresponding to concentrations of anti-Biofullerene antibody and the secondary antibody was processed by an ACT-II software. Inner dotted curve: nuclear outline. Outer dotted curve: cell outline. Scale bar = 10 μm. c: HaCaT cells were treated as in (a) except using anti-PVP–fullerene antiserum. The images are representatives of three independent experiments. Scale bar = 10 μm. [Color figure can be viewed in the online issue, which is available at wileyonlinelibrary.com]

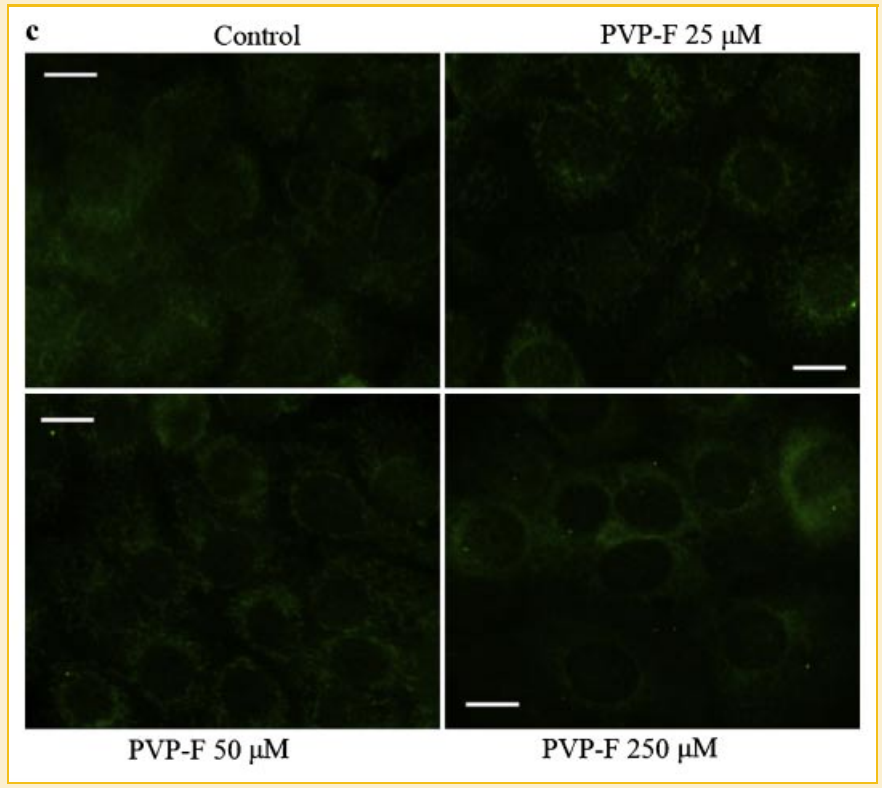

Fig. 2. (*Continued*)

UVA IRRADIATION

After the culture medium was removed, cells were irradiated, in 200–500 μl of PR-free DMEM containing no fullerene, with UV lamps. The samples were rinsed three times by PR-free DMEM before UVA irradiation. The emission maximum of the lamp was centered at 365 nm with sheltering of UVB ray by a silica glass filter. The control samples were kept in the dark under the same conditions. The effect of UVA irradiation on cell viability was evaluated by WST-1 assay according to the previous report [Xiao et al., 2005].

PI STAIN AND FLOW CYTOMETRY FOR APOPTOSIS-INDUCED CELLS

HaCaT cells were prepared according to the detailed protocol created by BECKMAN COULTER, Co. The cell cycle and intracellular DNA content were analyzed with a COULTER® EPICS® XL™ flow cytometer using EXPO32™ software (BECKMAN COULTER, Co.). Cells showing a DNA content less than the peak for G_1/G_0 were considered to be subdiploid and apoptotic. The fluorescence images were photographed under a fluorescence microscope (NIKON ECLIPSE E600). The wavelengths of excitation and emission were 485 and 530 nm, respectively.

TUNEL ASSAY AND FLOW CYTOMETRY FOR APOPTOSIS-INDUCED CELLS

The DNA fragments of NHEM cells were detected with TdT-mediated dUTP-FITC nick end labeling (TUNEL) method using the MEBSTAIN Apoptosis kit Direct (BECKMAN COULTER, Co.). Cells were prepared according to the detailed protocol and analyzed with a COULTER® EPICS® XL™ flow cytometer using EXPO32™ software (BECKMEN COULTER, Co.). The fluorescence intensity corresponding to extents of DNA cleavages was also evaluated with a fluorescence microscope (NIKON ECLIPSE E600) using an AquaCosmos software.

STATISTICAL ANALYSIS

All data, expressed as mean ± standard deviation, were processed statistically by the software of SPSS 11.5 for Windows. The differences of the data were considered significance when $P < 0.05$.

RESULTS

INTRACELLULAR DISTRIBUTION OF PVP–FULLERENE IN HaCaT CELLS

We prepared anti-Biofullerene and anti-PVP–fullerene antisera to detect the intracellular distribution of PVP–fullerene. As shown in Figure 2a at 3 h after incubation with PVP–fullerene of 25, 50, and 250 μM, the anti-Biofullerene antiserum-stained HaCaT cells showed the significant fluorescence with punctuated dots surrounding the nucleus, which suggested that fullerene particles could cross the cell membrane and locate in the cytoplasm and peri-nuclear regions. At 250 or 50 μM of PVP–fullerene, a fullerene-attributed slight or faint fluorescence was detected in the nucleus (the right-ended or second-right panel of Fig. 2b). The fullerene-attributed fluorescence intensity was increased in a dose-dependent manner.

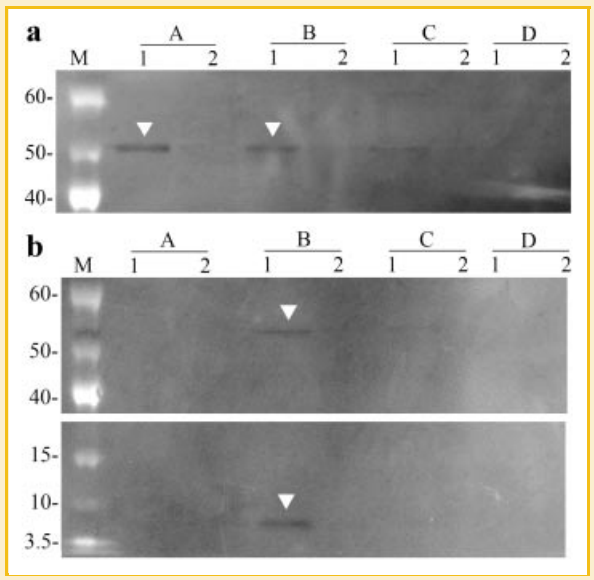

Fig. 3. Intracellular localization of PVP–fullerene and Biofullerene in HaCaT cells. HaCaT cells were incubated with PVP–fullerene at 250 μM for 3 h, and the extracts from 1×10^7 cells were fractionated to four subcellular components and subjected to immunoblots. Then the transferred membrane was immunostained with anti-Biofullerene (a) or anti-PVP–fullerene antiserum (b). The autoradiographic films were scanned and analyzed with an ACT-II software. The images are representatives of three independent experiments. The arrow heads indicate bands. M, molecular weight markers; 1, PVP–fullerene; 2, control; A, cytosol; B, membrane; C, nucleus; D, cytoskeleton.

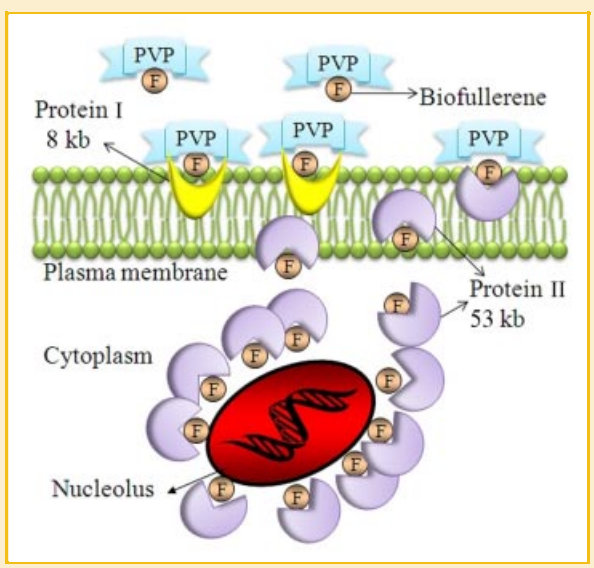

Fig. 4. The mechanism of permeation of PVP–fullerene into HaCaT cells. After administration with PVP–fullerenes to HaCaT cells for 3 h, PVP–fullerene clathrate compounds combine with protein I (8 kb), which localizes in the membrane, and protein II (53 kb), which localizes in the membrane and cytosol. Then the Biofullerene molecules are separated from the PVP–fullerene clathrate compounds and cross through the lipid-enriched membrane. Afterwards, the Biofullerene molecules conjugated protein II (53 kb) in the cytosol. Biofullerene molecules are scarce in the nucleus, and cannot combine with any proteins in the cytoskeleton. [Color figure can be viewed in the online issue, which is available at wileyonlinelibrary.com]

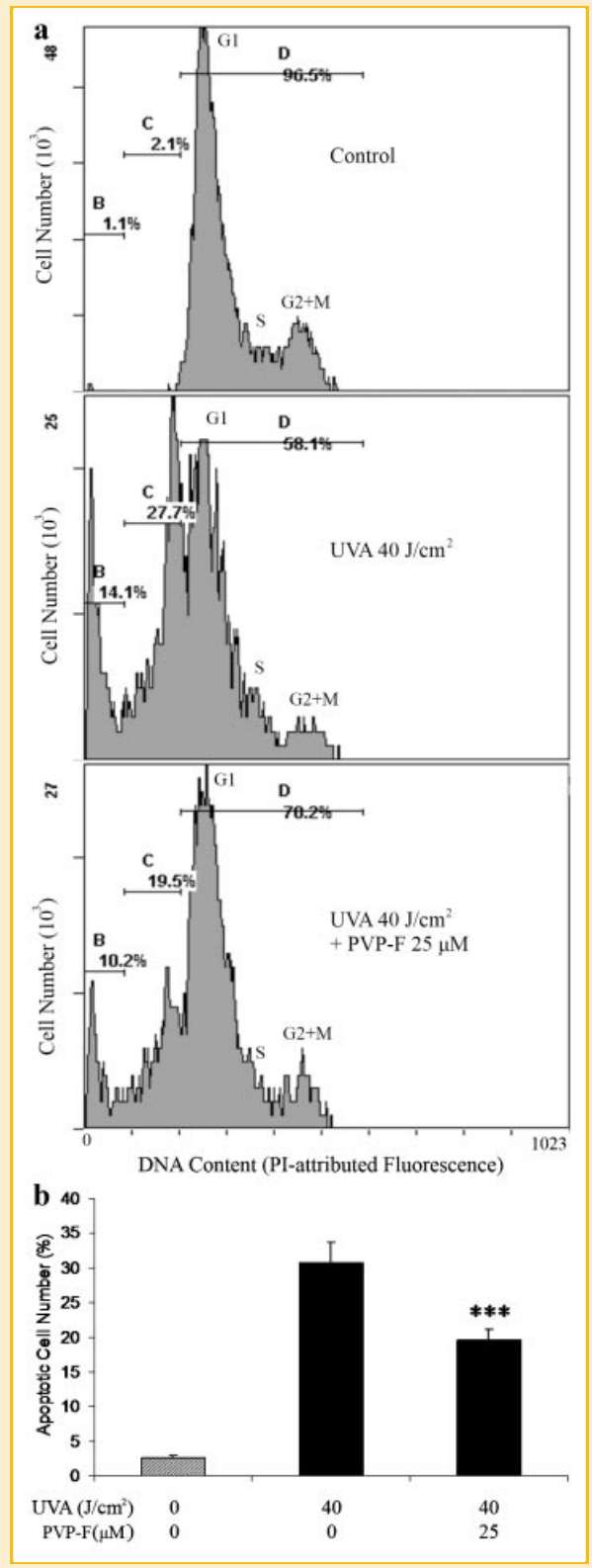

Fig. 5.

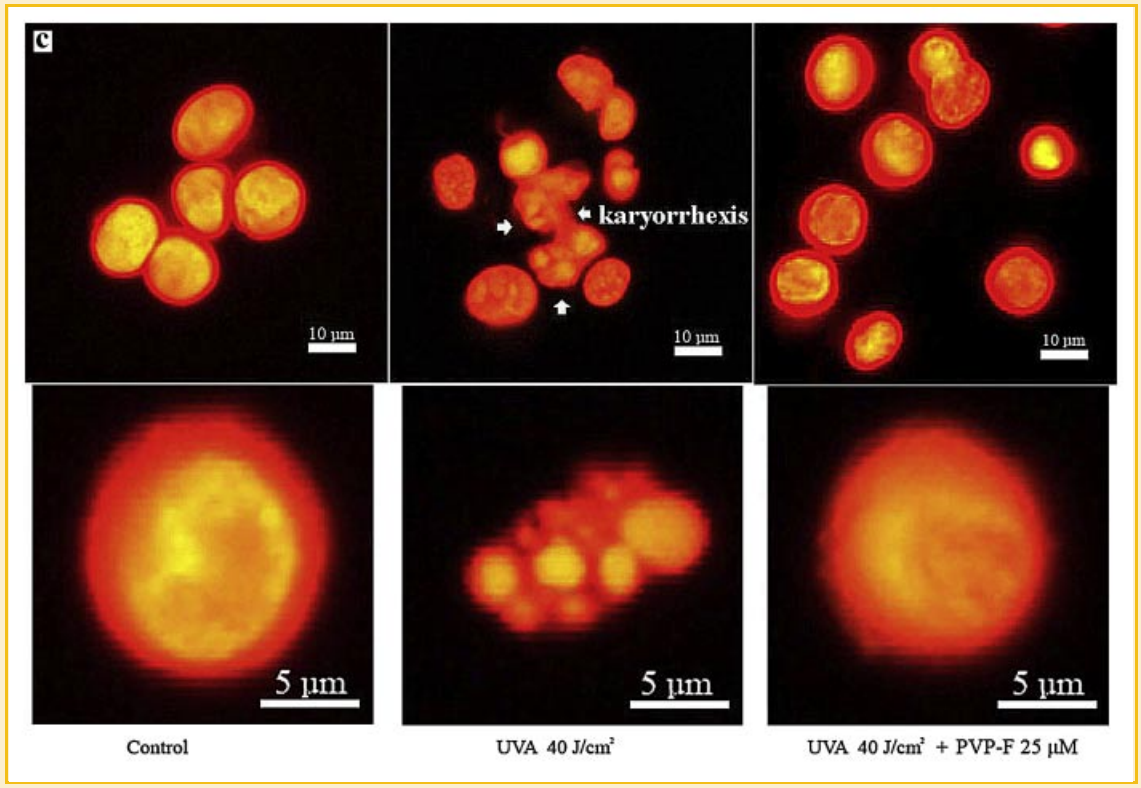

Fig. 5. Inhibitory effect of PVP–fullerene on UVA-induced apoptosis in HaCaT keratinocytes. a: Histograms from one representative flow cytometry experiment. HaCaT cells were seed in six-well plates at a density of 50,000 cells/well and cultivated for 18 h. At 3 h after incubation with or without PVP-fullerene at 25 μM, the cells were rinsed three times with PR-free DMEM and then irradiated using a UVA emission apparatus in 500 μl PR-free DMEM. Cells were further incubated for 12 h and then stained with PI. Out of them, 10,000 arbitrary cells were evaluated by single-parameter flow cytometry using PI fluorescence, and the typical data are expressed in a histogram. Fluorescence intensities are indicated in the logarithmic mode (*x*-axes). The data analysis was using an EXPO32^{TM} software. Area B: The percentages of dead cells. Area C: The percentages of apoptotic cells. Area D: The percentages of live cells (G_0/G_1, S, and G_2/M period). Cell fractions of G_1, S, and G_2 + M phases were 69 ± 4%, 11 ± 3%, and 16 ± 3% for "Control," 40 ± 3%, 10 ± 2%, and 8 ± 2% for "UVA 40 J/cm^2" and 46 ± 2%, 12 ± 3%, and 13 ± 1% for "UVA 40 J/cm^2 + RS 25 μM," respectively. b: Flow cytometric analysis for apoptotic changes of HaCaT cells receiving PI stain. Data are expressed as % of the total cells, and each column and bar represent the mean ± SD of five independent experiments. $^{***}P < 0.001$ versus "PVP–F 0 μM." c: Above-mentioned harvested cells were smeared on a slide glass and observed using a fluorescence microscopy NIKON ECLIPSE E600 (em: 450 nm; ex: 520 nm). Note the arrow-indicated karyorrhexis. [Color figure can be viewed in the online issue, which is available at wileyonlinelibrary.com]

In contrast, as compared with the control cells, only slender fluorescence could be detected in anti-PVP–fullerene antiserum-stained cells, which were incubated with PVP–fullerene even at 250 μM. There is no significant difference in fluorescence intensity, which is attributed assumedly to PVP moiety, among the control cells and cells treated with PVP–fullerene of 25 and 50 μM (Fig. 2c).

CELLULAR LOCALIZATION OF PVP–FULLERENE AND BIOFULLERENE IN HACAT CELLS

To understand how fullerene C60 molecules permeate into HaCaT cells, we extracted subcellular proteins of cytosol, membrane/organelle, nucleus, and cytoskeleton from adherent HaCaT cells, and then detected anti-Biofullerene antibody- and anti-PVP–fullerene antibody-binding sites by Western blotting analysis. As shown in Figure 3a after immunostained with anti-Biofullerene antibody, an obvious band was shown at the cytosol lane of PVP–fullerene sample at a 53-kb position. There was also another band at the membrane/organelle lane at a 53-kb position, however, it was much weaker than at the cytosol. The band at the nucleus lane was almost undetectable in PVP–fullerene sample. Interestingly anti-PVP–fullerene antibody-stained sample showed one obvious band and one weak band on the membrane/organelle lane of PVP–fullerene sample at 8 and 53 kb, respectively (Fig. 3b). There was no band in both anti-PVP–fullerene and anti-Biofullerene antibodies-stained control samples. These data suggest that PVP–fullerene is able to combine the 8- and 53-kb proteins which localize in the membrane of HaCaT kerytinocytes. Only fullerene molecules can cross the lipid membrane and conjugate 53 kb proteins in the cytosol and membrane (Fig. 4).

INHIBITORY EFFECT OF PVP–FULLERENE ON UVA-INDUCED APOPTOSIS IN HACAT KERATINOCYTES

We have demonstrated that PVP–fullerene could protect HaCaT keratinocytes from UVA-induced cell death, which remains to be analyzed for the underlying mechanism. Because the optimal cytoprotection of PVP–fullerene is achieved by administration at doses of 20–30 μM at 3 h before UVA irradiation [Xiao et al., 2006], we choose the concentration of 25 μM and 3-h preadministrations to test the anti-apoptotic effect of PVP–fullerene in the present studies. To investigate the cytoprotective ability of PVP–fullerene on HaCaT

keratinocytes, apoptosis was induced by irradiation with UVA (40 J/cm^2). At 12 h after UVA irradiation, HaCaT cells showed significant apoptosis, which was assessed by nuclear staining with PI fluorescent reagent, and analyzed by flow cytometry and fluorescence microscopy. As shown in Figure 5b the percentages of apoptotic cells detected by flow cytometric analysis showed that ~30% of the UVA-irradiated cells underwent apoptosis, whereas the presence of 25 μM of PVP–fullerene significantly decreased the numbers of apoptotic cells to ~19.6% ($P < 0.001$ vs. "PVP–fullerene 0 μM"). Histograms from one representative flow cytometry experiment showed that a proportion of HaCaT cells with a DNA content below diploidy was increased by UVA irradiation, which indicated that the cells underwent apoptosis. The $G_2 + M$ and S cell fractions were markedly decreased for the UVA-irradiated cells as compared with the control cells, suggesting UVA-attributed slowdown of the cell cycle and the concurrent lowering of DNA synthesis (Fig. 5a). In DNA-stained cultures that were irradiated with UVA, cellular morphological aspects such as cell shrinkage, nuclear fragmentation (karyorrhexis), and nuclear condensation (pyknosis) in part were observed (Fig. 5c, middle panel). The presence of PVP–fullerene blocked the UVA-induced cell morphological changes.

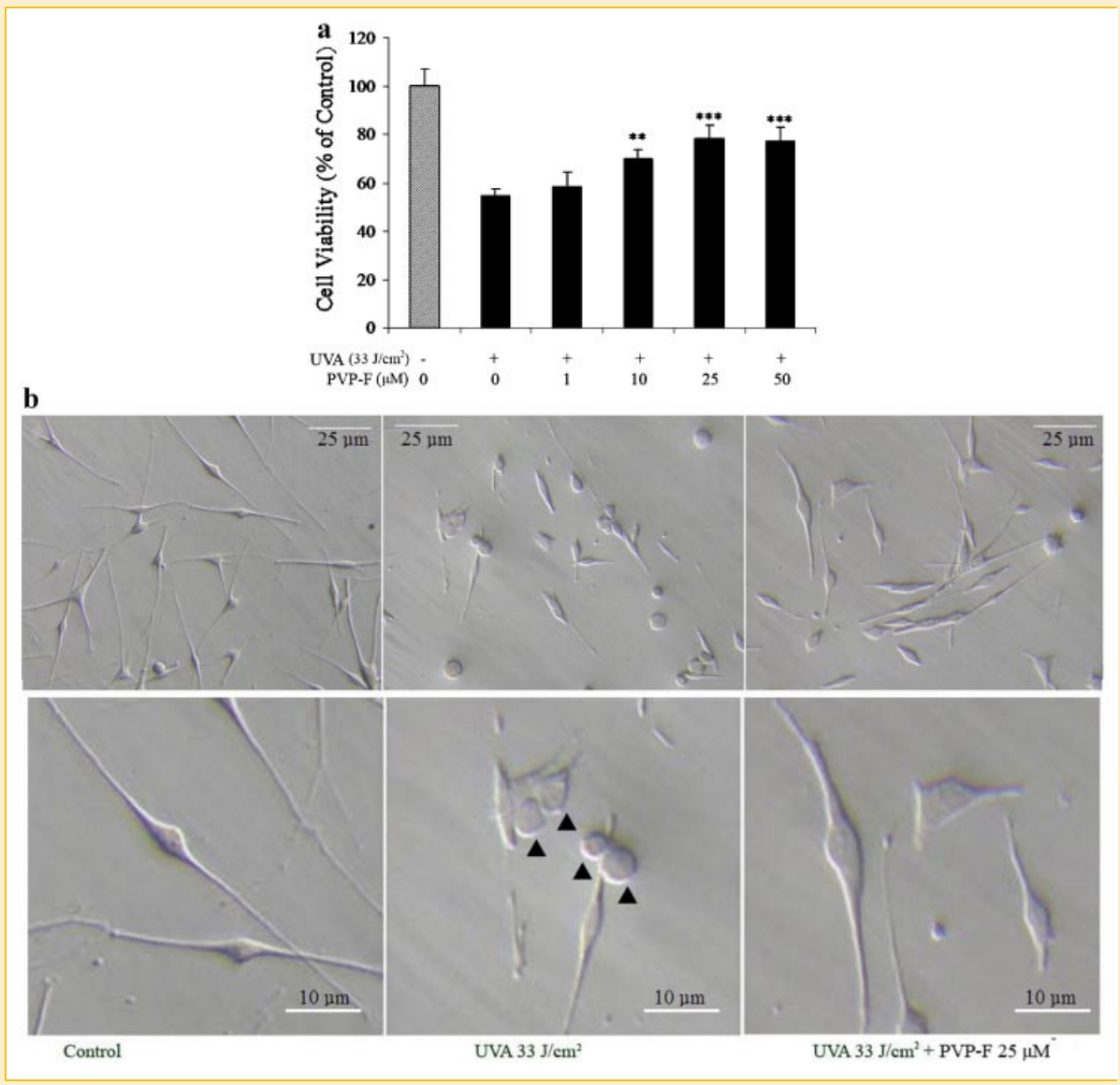

Fig. 6. Protective effect of PVP–fullerene against UVA-induced cell death in normal human epidermal melanocytes NHEM. a: NHEM cells were seed in 24-well plates at a density of 8,000 cells/well and cultivated for 18 h. At 3 h after incubation with or without PVP–fullerene at different concentrations, the cells were rinsed three times with PR-free DMEM and then irradiated using a UVA emission apparatus in 200 μl PR-free DMEM. Cells were further incubated for 48 h and then measured for the cell viability by mitochondrial dehydrogenase-based WST-1 assay. Data are expressed as % of the control, and each column and bar represent the mean ± SD of five independent experiments. $^{**}P < 0.01$; $^{***}P < 0.001$ versus "PVP–F 0 μM." b: Cultures of NHEM cells under above-mentioned conditions. The images were observed using a phase-contrast microcopy with a Hoffman interference apparatus (Nikon DM510). The arrow heads indicate apoptosis-like morphology. Scale bar = 25 μm.

PROTECTIVE EFFECT OF PVP–FULLERENE AGAINST UVA-INDUCED CELL DEATH IN NORMAL HUMAN MELANOCYTES NHEM

To examine the cytoprotective effects of PVP–fullerene in human melanocytes NHEM, cell death was induced by irradiation with UVA (33 J/cm^2). As shown in Figure 6b at 48 h after UVA irradiation, NHEM cells underwent severe morphological damages. The cells became rounded and detached from the plate substratum. UVA irradiation markedly decreased the cell viability to 54% of the control cells, whereas PVP–fullerene significantly restored the cell viability to 70–78% at the concentrations of 10–50 μM, especially markedly at 25 μM of PVP–fullerene (Fig. 6a), which was shown to be cytoprotective against UVA injuries to NHEM melanocytes.

INHIBITORY EFFECT OF PVP–FULLERENE ON UVA-INDUCED APOPTOSIS IN NHEM CELLS

We further tested the preventive effect of PVP–fullerene against UVA-induced DNA strand cleavages in human melanocytes NHEM by TUNEL assay using flow cytometric analysis. NHEM cells showed a higher tolerance to UVA than HaCaT keratinocytes. UVA irradiation at a higher irradiance of 50 J/cm^2 induced apoptosis for ~15% versus the total cells in NHEM melanocytes. The apoptotic percentage of PVP–fullerene (25 μM)-pretreated cells was markedly reduced to about 8% ($P < 0.001$ vs. non-treated cells) (Fig. 7b). Histograms from one representative flow cytometry experiment showed that, at 12 h after UVA irradiation, ~15% of NHEM cells showed more intense fluorescence which suggested those cells suffered from abundant DNA cleavages, whereas the control cells or PVP–fullerene-pretreated cells showed scarce DNA cleavages (Fig. 7a). Figure 7c showed that, after UVA irradiation, the characteristic intense nuclear stain (from blue to red in pseudo-color) due to FITC-conjugated dUTP which labeled the DNA stand cleavage terminals was observed in NHEM cells, whereas this fluorescent labeling was not shown in the presence of PVP–fullerene (25 μM). Thus PVP–fullerene was suggested to be able to rescue NHEM cells from apoptotic cell death.

INFLUENCE OF PVP–FULLERENE ON UVA-INDUCED TRANSLOCATION OF NF-kappaB p65-SUBUNIT FROM THE CYTOPLASM TO THE NUCLEUS IN HaCaT CELLS

To elucidate the effect of PVP–fullerene on cellular signaling pathway, the influence of PVP–fullerene on UVA-induced translocation of NF-kappaB was examined. ROS, which could be generated by UVA irradiation, enhanced the signal transduction pathways for NF-kappaB activation in the cytoplasm and the subsequent translocation into the nucleus [Tyrrell, 1996; Tak and Firestein, 2001]. Cellular NF-kappaB was determined with anti-NF-kappaB antibody using the immunofluorescence method. First, the relationship among UVA doses, past times, the expression degrees, and translocation of NF-kappaB was examined.

As shown in Figure 8a at 16 h after UVA irradiation (30 J/cm^2), the expression of NF-kappaB proteins was increased in the cytoplasm. The nuclear translocation occurred at 24 h after UVA irradiation. In contrast the UVA irradiation at a higher dose of 60 J/cm^2 induced morphological abnormalities and lower expression of NF-kappaB proteins in the cells. Based on this condition, we further investigated the influence of PVP–fullerene on NF-kappaB activity. Pretreatment of HaCaT cells with 25 μM PVP–fullerene for 3 h suppressed UVA (30 J/cm^2)-induced nuclear translocation of

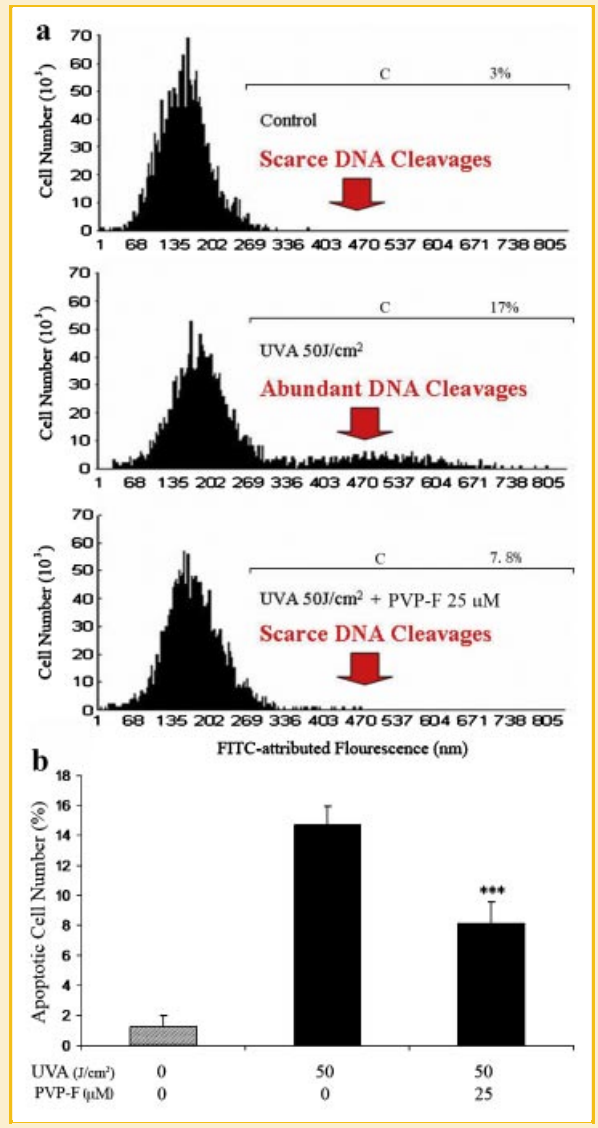

Fig. 7. Inhibitory effect of PVP–fullerene on UVA-induced DNA strand cleavages in NHEM cells. a: Histograms from one representative flow cytometry experiment. NHEM cells were treated as Figure 2 and then stained for the cellular DNA cleavage terminals by fluorescent dye-based TUNEL method. Out of them 10,000 arbitrary cells were evaluated by single-parameter flow cytometry using FITC fluorescence and expressed in a histogram. Fluorescence intensities are indicated in the logarithmic mode (*x*-axes). The data analysis was using an EXPO32^{TM} software. Area C: Percentages of apoptotic cells. b: Flow cytometric analysis for apoptotic changes of NHEM cells receiving TUNEL assay. Data are expressed as % of the total cells, and each column and bar represent the mean ± SD of five independent experiments. $^{***}P < 0.001$ versus "PVP–F 0 μM." c: Cells were treated as described in Figure 4a and smeared on a slide glass. Specimens were observed using a fluorescence microscopy NIKON ECLIPSE E600 (em: 450 nm; ex: 520 nm). The fluorescence intensity corresponding to extents of DNA cleavages was processed by an AquaCosmos software and expressed in a rainbow-colored gauge from blue (scarce DNA cleavages) to red (abundant DNA cleavages). Scale bar = 10 μm. [Color figure can be viewed in the online issue, which is available at wileyonlinelibrary.com]

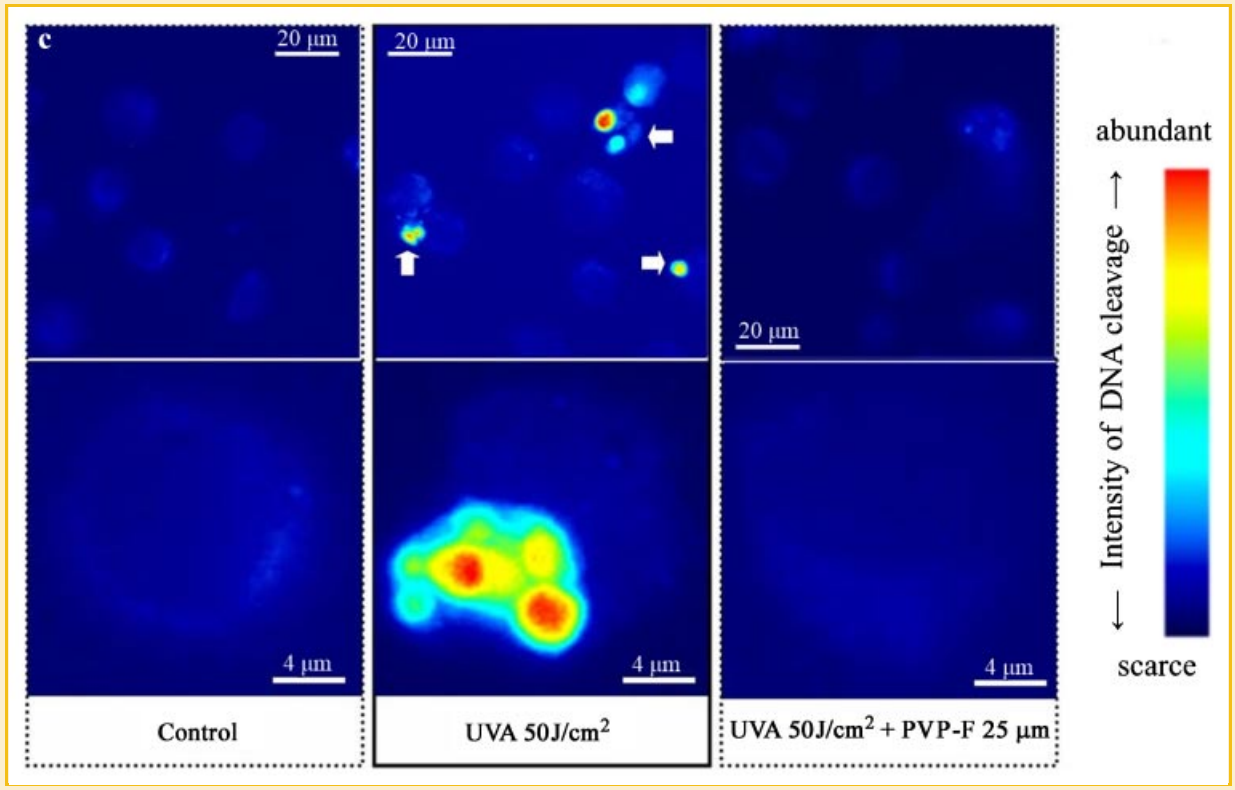

Fig. 7. (*Continued*)

NF-kappaB (Fig. 8b). These results suggested that PVP–fullerene exerts the anti-apoptotic effect through the influence to cellular apoptotic signal transduction pathway.

DISCUSSION

Fullerene C60 derivatives can be incorporated into artificial lipid bilayers [Hwang and Mauzerall, 1993], and rapidly accumulated into human keratinocytes or human fibroblasts without cytotoxicity [Scrivens et al., 1997]. Inside the cells, fullerene-C60 localizes preferentially to mitochondria [Foley et al., 2002], which generate the great mass of cellular ROS. Although fullerene and its derivatives are considered as antioxidants, it has been reported that several derivatives of fullerene showed cytotoxicity to some cell species at certain concentrations [Sayes et al., 2005]. In our previous study, we have screened out the fullerene-PVP clathrate as a safe and powerful antioxidant from several water-soluble derivatives of fullerene [Xiao et al., 2005, 2006]. In the present study, we first demonstrated that PVP–fullerene is able to combine the 8- and 53-kb proteins which localize in the membrane of HaCaT kerytinocytes. Only fullerene molecules are able to cross the lipid membrane, and conjugate 53-kb proteins in the cytosol. The immunofluorescence staining data showed that, after passing through the cytoplasmic membrane, Biofullerene molecules localize in cytoplasm surrounding the nucleus or in part in the nucleus. These findings suggest that PVP–fullerene clathrate and Biofullerene molecules might act like protectants to prevent ROS-induced membrane damage, especially nuclear membrane damage in the cell, and therefore stabilize cellular membranes against oxidative injuries. The whole PVP–fullerene molecule is not able to enter into the cells, which is considered that PVP–fullerene molecule was possibly separated into PVP and Biofullerene because fullerene may exert an appreciable affinity with lipid portion (it might be protein II) of the cell membrane, and subsequently cross the plasma membrane owing to lipophilic and smaller molecular properties in contrast to the hydrophilic and larger molecule PVP.

The oxidative stress generated by UVA irradiation causes DNA cleavage, and consequently activates NF-kappaB, which is one of the SOS responses in skin, related to multiple deleterious signaling pathways and reportedly plays important roles in photoaging and carcinogenesis [Muller et al., 1993; Kim et al., 2002; Kabe et al., 2005]. According to our data (Fig. 8a), the stronger UVA irradiation (60 J/cm^2) caused a serious damage to HaCaT cells which lost the cellular SOS responses and failed in the activation of NF-kappaB, whereas the translocation of NF-kappaB from the cytoplasm to the nucleus could be observed in HaCaT cells which were irradiated by UVA at a lower dose (30 J/cm^2). PVP–fullerene-pretreated cells did not show the translocation of NF-kappaB, indicating that the cellular abnormal inflammatory and immune signaling cascades might be prevented. From these evidences, the cytoprotection by PVP–fullerene against UVA irradiation is considered to be accompanied by DNA preservation against oxidative damages attributed to UVA-induced ROS, which can be scavenged by the fullerene derivative as demonstrated by fluorography using the redox indicator CDCFH-DA [Xiao et al., 2005, 2007].

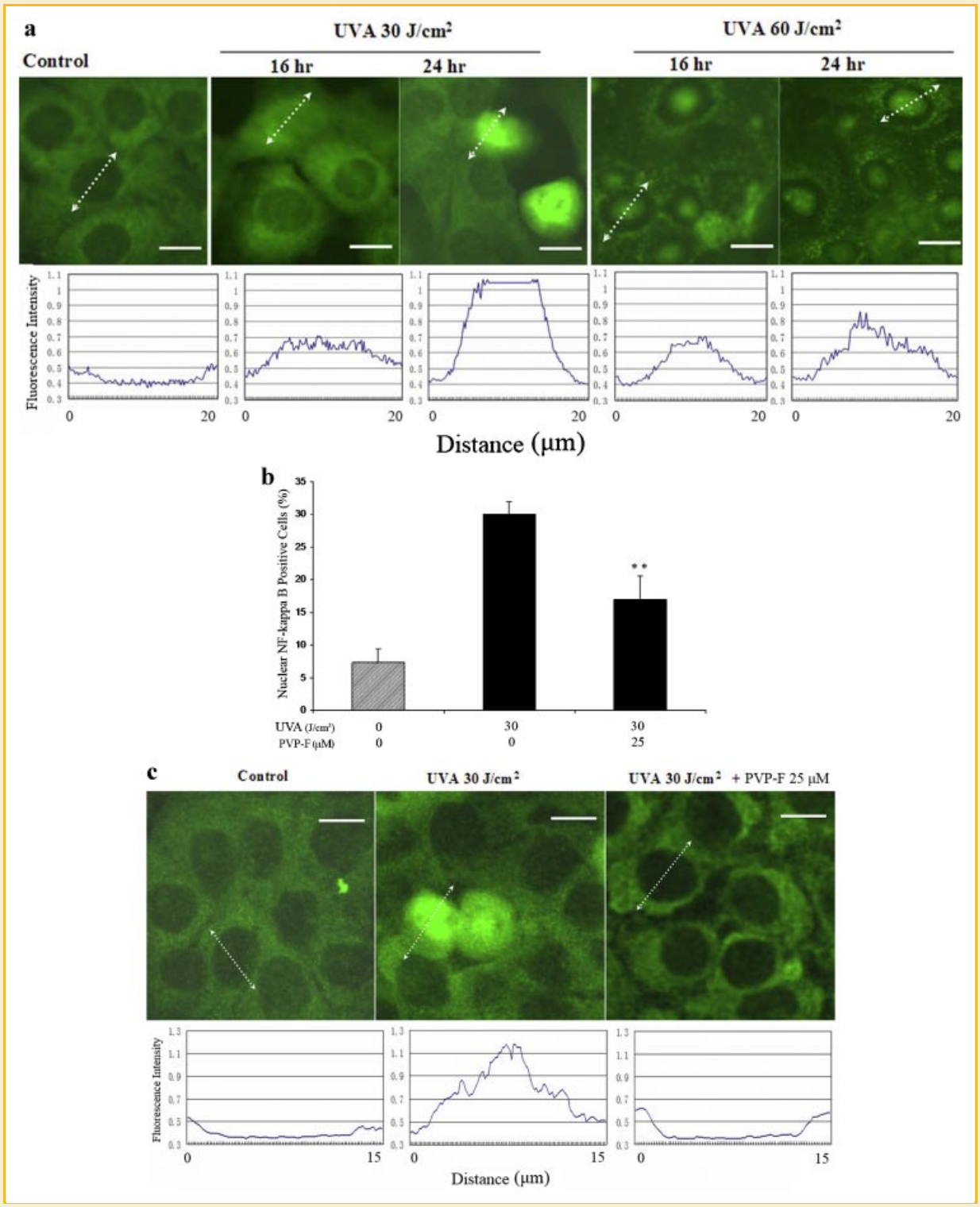

Fig. 8. Influence of PVP–fullerene on the translocation of NF-kappaB p65 from the cytoplasm to the nucleus in HaCaT cells. a: HaCaT cells were seeded on a chamber slide at a density of 8,000 cells/well and cultivated for 24 h. The cells were then irradiated with UVA at different doses in 200 μl PR-free DMEM. Cells were further incubated for 16–24 h and then immunostained with anti-NF-kappaB rabbit antibody and visualized with FITC-conjugated goat anti-rabbit IgG antibody. Specimens were observed with a fluorescence microscope. The histogram of the fluorescence intensity corresponding to extents of the nuclear expression of NF-kappaB proteins in a typical single cell shown in a dotted arrow line was processed by an AquaCosmos software. The images are representatives of three independent experiments. Scale bar = 10 μm. b: HaCaT cells were similarly seeded and cultivated. At 3 h after incubation with or without PVP–fullerene (25 μM), the cells were then irradiated with UVA at a dose of 30 J/cm^2 in 200 μl PR-free DMEM. Cells were further incubated for 24 h and then similarly immunostained. Specimens were observed under a fluorescence microscope. Out of 500 arbitrary cells, nuclear NF-kappaB-positive cells were counted with an ImageTool software. Data are expressed as % of the total cells, and each column and bar represent the mean ± SD of three independent experiments. $^{**}P < 0.01$ versus "PVP–F 0 μM." c: The images are representatives of three independent experiments. The histogram of the fluorescence intensity corresponding to extents of the nuclear expression of NF-kappaB proteins was processed by an AquaCosmos software. Scale bar = 10 μm. [Color figure can be viewed in the online issue, which is available at wileyonlinelibrary.com]

In conclusion, PVP–fullerene may act as an anti-apoptotic, UV-protective, and DNA-preservative agent, and is expected to be also potently developed as an anti-inflammatory and anti-photo-aging agent, through scavenging of intracellular ROS and an NF-kappaB-antagonist as the intrinsic action, in terms of the prevention of both skin aging and carcinogenesis.

REFERENCES

Ashok BT, Ahmad J, Ali R. 1998. Immunochemical detection of oxidative DNA damage in cancer and aging using anti-reactive oxygen species modified DNA monoclonal antibody. Int J Biochem Cell Biol 30:1367–1377.

Bedrov D, Smith GD, Davande H, Li L. 2008. Passive transport of C60 fullerenes through a lipid membrane: A molecular dynamics simulation study. J Phys Chem B 112:2078–2084.

Boukamp P, Petrussevska RT, Breitkreutz D, Hornung J, Markham A, Fusenig NE. 1988. Normal keratinization in a spontaneously immortalized aneuploid human keratinocyte cell line. J Cell Biol 106:761–771.

Chen BX, Wilson SR, Das M, Coughlin DJ, Erlanger BF. 1998. Antigenicity of fullerenes: Antibodies specific for fullerenes and their characteristics. Proc Natl Acad Sci USA 95:10809–10813.

Dugan LL, Gabrielsen JK, Yu SP, Lin TS, Choi DW. 1996. Buckminsterfullerenol free radical scavengers reduce excitotoxic and apoptotic death of cultured cortical neurons. Neurobiol Dis 3:129–135.

Foley S, Crowley C, Smaihi M, Bonfils C, Erlanger BF, Seta P, Larroque C. 2002. Cellular localisation of a water-soluble fullerene derivative. Biochem Biophys Res Commun 294:116–119.

Gan Q, Li T, Hu B, Lian M, Zheng X. 2009. HSCARG inhibits activation of NF-kappaB by interacting with IkappaB kinase-beta. J Cell Sci 122:4081–4088.

Hu Z, Guan W, Wang W, Huang L, Xing H, Zhu Z. 2007. Protective effect of a novel cystine C(60) derivative on hydrogen peroxide-induced apoptosis in rat pheochromocytoma PC12 cells. Chem Biol Interact 167:135–144.

Hwang KC, Mauzerall D. 1993. Photoinduced electron transport across a lipid bilayer mediated by C70. Nature 361:138–140.

Kabe Y, Ando K, Hirao S, Yoshida M, Handa H. 2005. Redox regulation of NF-kappaB activation: Distinct redox regulation between the cytoplasm and the nucleus. Antioxid Redox Signal 7:395–403.

Kim SJ, Hwang SG, Shin DY, Kang SS, Chun JS. 2002. p38 kinase regulates nitric oxide-induced apoptosis of articular chondrocytes by accumulating p53 via NFkappa B-dependent transcription and stabilization by serine 15 phosphorylation. J Biol Chem 277:33501–33508.

Kothny-Wilkes G, Kulms D, Pöppelmann B, Luger TA, Kubin M, Schwarz T. 1998. Interleukin-1 protects transformed keratinocytes from tumor necrosis factor-related apoptosis-inducing ligand. J Biol Chem 273:29247–29253.

Kothny-Wilkes G, Kulms D, Luger TA, Kubin M, Schwarz T. 1999. Interleukin-1 protects transformed keratinocytes from tumor necrosis factor-related apoptosis-inducing ligand- and CD95-induced apoptosis but not from ultraviolet radiation-induced apoptosis. J Biol Chem 274:28916–28921.

Krusic PJ, Wasserman E, Keizer PN, Morton JR, Preston KF. 1991. Radical reaction of C_{60}. Science 254:1183–1185.

Lao F, Chen L, Li W, Ge C, Qu Y, Sun Q, Zhao Y, Han D, Chen C. 2009. Fullerene nanoparticles selectively enter oxidation-damaged cerebral microvessel endothelial cells and inhibit JNK-related apoptosis. ACS Nano 3:3358–3368.

Lin AM, Chyi BY, Wang SD, Yu HH, Kanakamma PP, Luh TY, Chou CK, Ho LT. 1999. Carboxyfullerene prevents iron-induced oxidative stress in rat brain. J Neurochem 72:1634–1640.

Lipinski CA, Lombardo F, Dominy BW, Feeney PJ. 2001. Experimental and computational approaches to estimate solubility and permeability in drug discovery and development settings. Adv Drug Deliv Rev 46:3–26.

Muller JM, Ziegler-Heitbrock HW, Baeuerle PA. 1993. Nuclear factor kappa B, a mediator of lipopolysaccharide effects. Immunobiology 187:233–256.

Penna A, Cahalan M. 2007. Western blotting using the Invitrogen NuPage Novex Bis Tris minigels. J Vis Exp (7): 264.

Plantivaux A, Szegezdi E, Samali A, Egan L. 2009. Is there a role for nuclear factor kappaB in tumor necrosis factor-related apoptosis-inducing ligand resistance? Ann NY Acad Sci 1171:38–49.

Pöppelmann B, Klimmek K, Strozyk E, Voss R, Schwarz T, Kulms D. 2005. NF-κB-dependent down-regulation of tumor necrosis factor receptor-associated proteins contributes to interleukin-1-mediated enhancement of ultraviolet B-induced apoptosis. J Biol Chem 280:15635–15643.

Porter AE, Muller K, Skepper J, Midgley P, Welland M. 2006. Uptake of C60 by human monocyte macrophages, its localization and implications for toxicity: Studied by high resolution electron microscopy and electron tomography. Acta Biomater 2:409–419.

Quick KL, Ali SS, Arch R, Xiong C, Wozniak D, Dugan LL. 2008. A carboxyfullerene SOD mimetic improves cognition and extends the lifespan of mice. Neurobiol Aging 29:117–128.

Reelfs O, Tyrrell RM, Pourzand C. 2004. Ultraviolet a radiation-induced immediate iron release is a key modulator of the activation of NF-kappaB in human skin fibroblasts. J Invest Dermatol 122:1440–1447.

Ridley AJ, Whiteside JR, McMillan TJ, Allinson SL. 2009. Cellular and subcellular responses to UVA in relation to carcinogenesis. Int J Radiat Biol 85:177–195.

Sayes CM, Gobin AM, Ausman KD, Mendez J, West JL, Colvin VL. 2005. Nano-C60 cytotoxicity is due to lipid peroxidation. Biomaterials 26:7587–7595.

Scrivens WA, Rawlett AM, Tour JM. 1997. Preparative benchtop enrichment of C(60), C(70), and the higher fullerene allotropes using a brominated polystyrene stationary phase. J Org Chem 62:2310–2311.

Strozyk E, Pöppelmann B, Schwarz T, Kulms D. 2006. Differential effects of NF-kappaB on apoptosis induced by DNA-damaging agents: The type of DNA damage determines the final outcome. Oncogene 25:6239–6251.

Tak PP, Firestein GS. 2001. NF-kappaB: A key role in inflammatory diseases. J Clin Invest 107:7–11.

Testa U. 2010. TRAIL/TRAIL-R in hematologic malignancies. J Cell Biochem 110:21–34.

Tyrrell RM. 1996. Activation of mammalian gene expression by the UV component of sunlight—From models to reality. Bioessays 18:139–148.

Valko M, Leibfritz D, Moncol J, Cronin MT, Mazur M, Telser J. 2007. Free radicals and antioxidants in normal physiological functions and human disease. Int J Biochem Cell Biol 39:44–84.

Wang IC, Tai LA, Lee DD, Kanakamma PP, Shen CK, Luh TY, Cheng CH, Hwang KC. 1999. C(60) and water-soluble fullerene derivatives as antioxidants against radical-initiated lipid peroxidation. J Med Chem 42:4614–4620.

Witte P, Beuerle F, Hartnagel U, Lebovitz R, Savouchkina A, Sali S, Guldi D, Chronakis N, Hirsch A. 2007. Water solubility, antioxidant activity and cytochrome C binding of four families of exohedral adducts of C60 and C70. Org Biomol Chem 5:3599–3613.

Wong-Ekkabut J, Baoukina S, Triampo W, Tang IM, Tieleman DP, Monticelli L. 2008. Computer simulation study of fullerene translocation through lipid membranes. Nat Nanotechnol 3:363–368.

Xiao L, Takada H, Maeda K, Haramoto M, Miwa N. 2005. Antioxidant effects of water-soluble fullerene derivatives against ultraviolet ray or peroxylipid through their action of scavenging the reactive oxygen species in human skin keratinocytes. Biomed Pharmacother 59:351–358.

Xiao L, Takada H, Gan X, Miwa N. 2006. The water-soluble fullerene derivative "Radical Sponge" exerts cytoprotective action against UVA irradiation but not visible-light-catalyzed cytotoxicity in human skin keratinocytes. Bioorg Med Chem Lett 16:1590–1595.

Xiao L, Matsubayashi K, Miwa N. 2007. Inhibitory effect of the water-soluble polymer-wrapped derivative of fullerene on UVA-induced melanogenesis via downregulation of tyrosinase expression in human melanocytes and skin tissues. Arch Dermatol Res 299:245–257.

Xiao L, Aoshima H, Saitoh Y, Miwa N. 2010. The effect of squalane-dissolved fullerene-C60 on adipogenesis-accompanied oxidative stress and macrophage activation in a preadipocyte-monocyte co-culture system. Biomaterials 31:5976–5985.

Yamago S, Tokuyama H, Nakamura E, Kikuchi K, Kananishi S, Sueki K, Nakahara H, Enomoto S, Ambe F. 1995. In vivo biological behavior of a water-miscible fullerene: 14C labeling, absorption, distribution, excretion and acute toxicity. Chem Biol 2:385–389.

Yanada S, Misumi M, Saitoh Y, Kaneda Y, Miwa N. 2006. Transfection of the anti-apoptotic gene bcl-2 inhibits oxidative stress-induced cell injuries through delaying of NF-κB activation. Gene Ther Mol Biol 10: 269–276.

Yin JJ, Lao F, Fu PP, Wamer WG, Zhao Y, Wang PC, Qiu Y, Sun B, Xing G, Dong J, Liang XJ, Chen C. 2009. The scavenging of reactive oxygen species and the potential for cell protection by functionalized fullerene materials. Biomaterials 30:611–621.